Available online at www.sciencedirect.com
SCIENCE @ DIRECT®

C. R. Acad. Sci. Paris, Ser. I 336 (2003) 779–784

COMPTES RENDUS MATHEMATIQUE

Numerical Analysis

Numerical solution of the two-dimensional elliptic Monge–Ampère equation with Dirichlet boundary conditions: an augmented Lagrangian approach

Edward J. Dean, Roland Glowinski

Department of Mathematics, University of Houston, Houston, TX 77204-3008, USA

Received 7 January 2003; accepted 14 January 2003

Presented by Philippe G. Ciarlet

Abstract

The main goal of this Note is to discuss a method for the numerical solution of the two-dimensional elliptic Monge–Ampère equation with Dirichlet boundary conditions (the E-MAD problem). This method relies on the reformulation of E-MAD as a problem of Calculus of Variation involving the biharmonic operator (or closely related operators), and then to a saddle-point formulation for a well-chosen augmented Lagrangian functional, leading to iterative methods such as Uzawa–Douglas–Rachford. The above methodology applies to problems other than E-MAD (such as the Pucci equation). The results of numerical experiments are presented. They concern the solution of E-MAD on the unit square $(0,1)\times(0,1)$; the first test problem has a known smooth closed form solution which is easily computed with optimal order of convergence. The second test problem has also a known closed form solution; the fact that this solution has the $H^2(\Omega)$-regularity, but not the $C^2(\overline{\Omega})$ one, does not prevent optimal order of convergence. Finally, the third test problem having no smooth solution is more costly to solve and leads to discrete solutions showing negative curvature near the corners. ***To cite this article: E.J. Dean, R. Glowinski, C. R. Acad. Sci. Paris, Ser. I 336 (2003).***

Résumé

Une méthode de lagrangien augmenté pour la résolution numérique du problème de Monge–Ampère elliptique en dimension deux avec conditions de Dirichlet. L'objet essentiel de cette Note est l'étude d'une méthode pour la résolution numérique du problème de Dirichlet pour l'équation de Monge–Ampère elliptique en dimension deux (le problème E-MAD). Cette méthode repose sur une reformulation de E-MAD comme un problème de Calcul des Variations impliquant l'opérateur bi-harmonique (ou des opérateurs voisins), puis sur une formulation de type point-selle pour un Lagrangien augmenté bien choisi, ce qui conduit naturellement à des algorithmes du type Uzawa–Douglas–Rachford. La méthodologie ci-dessus s'applique à des problèmes autres que E-MAD (l'équation de Pucci, par exemple). Les résultats d'essais numériques sont egalement presentés. Ils concernent la résolution du problème E-MAD sur le carré unité $(0,1)\times(0,1)$. Le premier problème test a une solution régulière (analytique, en fait) connue exactement ; on la retrouve facilement, avec une erreur d'approximation d'ordre optimal. La solution du second probleme test est aussi connue exactement ; le fait qu'elle soit dans $H^2(\Omega)$ sans être dans $C^2(\overline{\Omega})$ n'empêche pas d'obtenir une erreur d'approximation d'ordre optimal. Finalement, le troisième problème test n'ayant pas de

E-mail addresses: dean@math.uh.edu (E.J. Dean), roland@math.uh.edu (R. Glowinski).

1631-073X/03/$ – see front matter
doi:10.1016/S1631-073X(03)00149-3

solution régulière est plus difficile à résoudre ; les solutions approchées obtenues montrent que la courbure devient negative au voisinage des coins. ***Pour citer cet article : E.J. Dean, R. Glowinski, C. R. Acad. Sci. Paris, Ser. I 336 (2003).***

1. Introduction

Let Ω be a bounded domain of $\mathbb{R}^d$ $(d \geqslant 2)$; the *Monge–Ampère equation*

$$\det D^2\psi = f \quad \text{in } \Omega, \tag{1}$$

with $D^2\psi = (\partial^2\psi/\partial x_i \partial x_j)_{1\leqslant i,j\leqslant d}$, has always been a source of interest for differential geometers (see, e.g., [1]); it has more recently attracted the interest of the *nonlinear partial differential equations* community, basic references being, e.g., [3,2]. The main goal of this Note is to address the numerical solution of the *two-dimensional elliptic* (i.e., $f > 0$ on Ω) *Monge–Ampère Dirichlet* (E-MAD) problem. The approach to be investigated relies on the reformulation of E-MAD as a problem from the *Calculus of Variations* involving the biharmonic operator Δ^2 (or closely related operators). The first approach takes advantage of a *saddle-point formulation* for a well-chosen *augmented Lagrangian functional*, leading to *Uzawa–Douglas–Rachford* algorithms, for example. A most interesting feature of the augmented Lagrangian approach is that “it seems” to provide a kind of generalized solution in $H^2(\Omega)$ even if the E-MAD problem under consideration has no solution in that space.

2. Formulation of the Dirichlet problem for the elliptic Monge–Ampère equation in dimension 2

Let Ω be a bounded domain of $\mathbb{R}^2$; we denote by Γ the boundary of Ω. The E-MAD problem can be written as follows:

$$\begin{cases} \det D^2\psi = f & \text{in } \Omega, \\ \psi = g & \text{on } \Gamma, \end{cases} \tag{E-MAD}$$

where $D^2\psi$ is the Hessian of ψ and where f and g are two given functions, with $f > 0$. Unlike the closely-related Dirichlet problem for the Laplace operator, E-MAD may have *multiple solutions*, and the *smoothness* of the data does not imply the existence of a smooth solution. Concerning the last property, suppose that $\Omega = (0,1) \times (0,1)$ and consider the particular E-MAD problem defined by

$$\frac{\partial^2\psi}{\partial x_1^2}\frac{\partial^2\psi}{\partial x_2^2} - \left|\frac{\partial^2\psi}{\partial x_1 \partial x_2}\right|^2 = 1 \quad \text{in } \Omega, \qquad \psi = 0 \quad \text{on } \Gamma. \tag{2}$$

Problem (2) cannot have smooth solutions since for those solutions the boundary condition $\psi = 0$ on Γ implies that $\frac{\partial^2\psi}{\partial x_1^2}\frac{\partial^2\psi}{\partial x_2^2}$ and $\frac{\partial^2\psi}{\partial x_1 \partial x_2}$ vanish at the boundary. Actually, the above (negative) result is not a consequence of the non-smoothness of Γ, since the above non-existence result persists if one replaces the above Ω by the ovoid-shaped domain whose C^∞-boundary is defined by $\Gamma = \bigcup_{i=1}^4 \Gamma_i$, with $\Gamma_1 = \{x \mid x = \{x_1, x_2\},\, x_2 = 0,\, 0 \leqslant x_1 \leqslant 1\}$, $\Gamma_3 = \{x \mid x = \{x_1, x_2\},\ x_2 = 1,\ 0 \leqslant x_1 \leqslant 1\}$, $\Gamma_2 = \{x \mid x = \{x_1, x_2\},\ x_1 = 1 + \mathrm{e}^{4-1/x_2(1-x_2)},\ 0 < x_2 < 1\}$, $\Gamma_4 = \{x \mid x = \{x_1, x_2\}, x_1 = -\mathrm{e}^{4-1/x_2(1-x_2)}, 0 < x_2 < 1\}$.

3. A saddle-point formulation of problem E-MAD. Related augmented Lagrangian iterative methods

The simplest Hilbert space where to solve problem E-MAD is clearly $H^2(\Omega)$. This leads us to introduce

$$V_g = \left\{\varphi \mid \varphi \in H^2(\Omega),\ \varphi = g \text{ on } \Gamma\right\}; \tag{3}$$

if $g \in H^{3/2}(\Gamma)$, the (affine) space V_g is non-empty. Assuming that E-MAD has solutions in V_g, it makes sense to consider the following problem from *Calculus of Variations*:

$$\psi \in E_g; \quad J_0(\psi) \leqslant J_0(\varphi), \quad \forall \varphi \in E_g, \tag{4}$$

where $J_0(\varphi) = \frac{1}{2}\int_\Omega |\Delta\varphi|^2\,dx$ and $E_g = \{\varphi \mid \varphi \in V_g, \det D^2\varphi = f\}$. Replacing $|\Delta\varphi|^2$ by $|D^2\varphi|^2$ in $J_0(\cdot)$, would work as well (above $|D^2\varphi| = \big(\sum_{1\leqslant i,j\leqslant 2}\big|\frac{\partial^2\varphi}{\partial x_i \partial x_j}\big|^2\big)^{1/2}$). Motivated by previous work on *nonlinear biharmonic problems* (see, e.g., [7,6,4]) we introduce the *symmetric tensor-valued functions* $\mathbf{p} = D^2\psi$, $\mathbf{q} = D^2\varphi$ and the related (equivalent to (4)) minimization problem:

$$j_0(\psi, \mathbf{p}) \leqslant j_0(\varphi, \mathbf{q}), \quad \forall \{\varphi, \mathbf{q}\} \in \mathcal{E}_g,\ \{\psi, \mathbf{p}\} \in \mathcal{E}_g, \tag{5}$$

where $j_0(\varphi, q) = (1/2)\int_\Omega |\Delta\varphi|^2\,dx$ and $\mathcal{E}_g = \{\{\varphi, \mathbf{q}\} \mid \varphi \in V_g,\ \mathbf{q} \in Q,\ \mathbf{q} = D^2\varphi,\ \det \mathbf{q} = f\}$, and $Q = \{\mathbf{q} \mid \mathbf{q} = (q_{ij})_{1\leqslant i,j\leqslant 2},\ q_{12} = q_{21},\ q_{ij} \in L^2(\Omega)\}$. Let r be a *positive* parameter; we associate to (5) the following *saddle-point problem*

$$\begin{cases} \mathcal{L}_r(\psi, \mathbf{p}; \boldsymbol{\mu}) \leqslant \mathcal{L}_r(\psi, \mathbf{p}; \boldsymbol{\lambda}) \leqslant \mathcal{L}_r(\varphi, \mathbf{q}; \boldsymbol{\lambda}), \quad \forall \big\{\{\varphi, \mathbf{q}\}, \boldsymbol{\mu}\big\} \in (V_g \times Q_f) \times Q, \\ \big\{\{\psi, \mathbf{p}\}, \boldsymbol{\lambda}\big\} \in (V_g \times Q_f) \times Q, \end{cases} \tag{6}$$

where $Q_f = \{\mathbf{q} \mid \mathbf{q} \in Q,\ \det \mathbf{q} = f\}$ and

$$\mathcal{L}_r(\varphi, \mathbf{q}; \boldsymbol{\mu}) = \frac{1}{2}\int_\Omega |\Delta\varphi|^2\,dx + \frac{r}{2}\int_\Omega \big|D^2\varphi - \mathbf{q}\big|^2\,dx + \int_\Omega \boldsymbol{\mu} : \big(D^2\varphi - \mathbf{q}\big)\,dx, \tag{7}$$

with $\mathbf{S} : \mathbf{T} = \sum_{1\leqslant i,j\leqslant 2} s_{ij}t_{ij}$ if $\mathbf{S} = (s_{ij})$ and $\mathbf{T} = (t_{ij})$. Suppose that problem (6) has a solution $\{\{\psi, \mathbf{p}\}, \boldsymbol{\lambda}\}$, then $\{\psi, \mathbf{p}\}$ is also a solution of (5). To compute the saddle-points of the *augmented Lagrangian* functional $\mathcal{L}_r$ we advocate (among other algorithms and because of its simplicity) the following Uzawa–Douglas–Rachford iterative method:

$$\big\{\psi^{-1}, \boldsymbol{\lambda}^0\big\} \quad \text{is given in } V_g \times Q; \tag{8}$$

then, for $n \geqslant 0$, $\{\psi^{n-1}, \boldsymbol{\lambda}^n\}$ *being known in* $V_g \times Q$*, solve*

$$\mathcal{L}_r\big(\psi^{n-1}, \mathbf{p}^n; \boldsymbol{\lambda}^n\big) \leqslant \mathcal{L}_r\big(\psi^{n-1}, \mathbf{q}; \boldsymbol{\lambda}^n\big), \quad \forall \mathbf{q} \in Q_f,\ \mathbf{p}^n \in Q_f, \tag{9}$$

$$\mathcal{L}_r\big(\psi^n, \mathbf{p}^n; \boldsymbol{\lambda}^n\big) \leqslant \mathcal{L}_r\big(\varphi, \mathbf{p}^n; \boldsymbol{\lambda}^n\big), \quad \forall \varphi \in V_g,\ \psi^n \in V_g, \tag{10}$$

$$\boldsymbol{\lambda}^{n+1} = \boldsymbol{\lambda}^n + r\big(D^2\psi^n - \mathbf{p}^n\big). \tag{11}$$

It follows from (7) that: (i) Problem (9) can be solved pointwise; to obtain $\mathbf{p}^n$ from ψ^{n-1} and $\boldsymbol{\lambda}^n$ we have to minimize, pointwise on Ω, a three-variable polynomial of the following type $\mathbf{z} = \{z_i\}_{i=1}^3 \to \frac{r}{2}(z_1^2 + z_2^2 + 2z_3^2) - \mathbf{b}_n(x)\cdot\mathbf{z}$ over the set defined by $z_1z_2 - z_3^2 = f(x)$. The above problem is a *generalized eigenvalue problem* which is solved by a variant of the *Newton's method.* (ii) Problem (10) is equivalent to a *well-posed linear variational problem* which reads as follows (with $V_0 = H^2(\Omega) \cap H_0^1(\Omega)$):

$$\int_\Omega \Delta\psi^n \Delta\varphi\,dx + r\int_\Omega D^2\psi^n : D^2\varphi\,dx = L_n(\varphi), \quad \forall \varphi \in V_0,\ \psi^n \in V_g, \tag{12}$$

with $L_n \in V_0'$. Problem (12) can be solved by a conjugate gradient algorithm operating in V_g (in fact in V_0) equipped with the scalar product $\{v, w\} \to \int_\Omega \Delta v \Delta w\,dx$. Each iteration requires the solution of two Poisson problems with Dirichlet boundary conditions. For the space approximation of problem (6) we have used a *mixed finite element discretization* closely related to the one employed in [7,6,4] for the numerical simulation of two-dimensional *Bingham visco-plastic flow* using the *stream function* formulation and – like here – augmented Lagrangian based iterative methods; with this approach, φ, $\mathbf{q}$, ψ, $\mathbf{p}$ are approximated by continuous piecewise linear approximations associated to a finite element triangulation of Ω. The condition $\det \mathbf{q} = f$ is imposed on the vertices of this triangulation.

Remark 3.1. Concerning the *initialization* of algorithm (8)–(11), we took $\boldsymbol{\lambda}^0 = \mathbf{0}$ and ψ^{-1} as the solution of $-\Delta\psi^{-1} = f^{1/2}$ in Ω, $\psi^{-1} = g$ on Γ.

Remark 3.2. If the continuous problem E-MAD has no smooth solution (like it is the case for problem (2)), we can expect the discrete analogue of $\mathcal{E}_g$ to be empty; in that case (this is true for linear saddle point problems, as shown in [7,5]) we expect the sequence $\{\boldsymbol{\lambda}_h^n\}_{n\geqslant 0}$ to diverge (arithmetically), while $\{\psi_h^n, \mathbf{p}_h^n\}$ will converge (geometrically) to a solution of *minimal norm* in the set $\{\{\varphi_h, \mathbf{q}_h\} \mid \varphi_h \in V_{g,h}, \mathbf{q}_h \in Q_{f,h}, \|D^2\varphi_h - \mathbf{q}_h\|_{L^2}$ is minimal$\}$, i.e., if $\mathcal{E}_{g,h}$ is empty, algorithm (8)–(11) solve the discrete E-MAD problem in a *least squares sense*. This suggests to look for least squares based methods for the solution of E-MAD; we are presently investigating such an approach.

Remark 3.3. The *numerical solution* of the *Monge–Ampère equations* has been addressed in [5]; the methods in [5] are "highly" *geometrical* in contrast to the *variational* one discussed in this Note which can be applied to a large variety of PDE problems from *Differential Geometry.*

4. Numerical experiments

The method discussed in Section 3 has been applied to the solution of three E-MAD test problems with $\Omega = (0,1)^2$. The *first test problem* can be expresed as follows:

$$\det D^2\psi = \left(1+\rho^2\right) \mathrm{e}^{\rho^2} \quad \text{in } \Omega, \qquad \varphi = g \quad \text{on } \Gamma, \tag{13}$$

with $\rho^2 = x_1^2 + x_2^2$ and g given by $g(x) = \mathrm{e}^{x_1^2/2}$ on $\{x \mid 0 < x_1 < 1,\ x_2 = 0\}$, $g(x) = \mathrm{e}^{x_2^2/2}$ on $\{x \mid x_1 = 0,\ 0 < x_2 < 1\}$, $g(x) = \mathrm{e}^{(1+x_1^2)/2}$ on $\{x \mid 0 < x_1 < 1,\ x_2 = 1\}$ and $g(x) = \mathrm{e}^{(1+x_2^2)/2}$ on $\{x \mid x_1 = 1,\ 0 < x_2 < 1\}$. The exact solution of (13) is given by $\psi(x_1, x_2) = \mathrm{e}^{\rho^2/2}$. We have discretized problem (13) relying on a mixed variational formulation, like the one discussed in [7,6,4], and used uniform triangulations of Ω, allowing us to solve the various elliptic problems encountered at each iteration of (8)–(11) by fast Poisson and Helmholtz solvers taking advantage of decomposition properties of biharmonic problems such as (12). Using as initial guess the approximate solutions of $-\Delta\varphi = \mathrm{e}^{\rho^2/2}\sqrt{1+\rho^2}$ in Ω, $\varphi = g$ on Γ, quite accurate approximations of the exact solution are obtained (employing $r = 1$ in (8)–(11)). After 100 iterations, $\|\psi_h^c - \psi\|_{L^2(\Omega)}$ is 2.6×10^{-5}, 6.7×10^{-6} and 1.8×10^{-6} for $h = 1/32$, $1/64$, and $1/128$, respectively (here ψ_h^c is the computed approximate solution); the $L^2(\Omega)$-approximation error is clearly $\mathrm{O}(h^2)$. Similar (good) performances are obtained when f and g correspond to smooth functions ψ known in advance. The computed approximate solution obtained by (8)–(11) with $h = 1/128$ has been visualized on Fig. 1.

The *second test problem* is-in some sense-more interesting, since it corresponds to a situation where E-MAD has a solution in $H^2(\Omega)$ which does not belong to $C^2(\overline{\Omega})$. To be more precise, consider the particular E-MAD problem defined by:

$$\det D^2\psi = \frac{1}{\rho} \quad \text{in } \Omega, \qquad \psi = g \quad \text{on } \Gamma \tag{14}$$

with ρ as above and g given by $g(x) = (2\sqrt{2}/3)x_1^{3/2}$ on $\{x \mid 0 < x_1 < 1,\ x_2 = 0\}$, $g(x) = (2\sqrt{2}/3)x_2^{3/2}$ on $\{x \mid x_1 = 0,\ 0 < x_2 < 1\}$, $g(x) = (2\sqrt{2}/3)(1+x_1^2)^{3/4}$ on $\{x \mid 0 < x_1 < 1,\ x_2 = 1\}$, and $g(x) = (2\sqrt{2}/3)(1+x_2^2)^{3/4}$ on $\{x \mid x_1 = 1,\ 0 < x_2 < 1\}$. With these data, ψ defined by $\psi(x_1, x_2) = (2\sqrt{2}/3)\rho^{3/2}$ is an exact solution of problem (14). We can easily show that the above function ψ belongs to $W^{2,p}(\Omega)$ if $p < 4$, but it does not have the

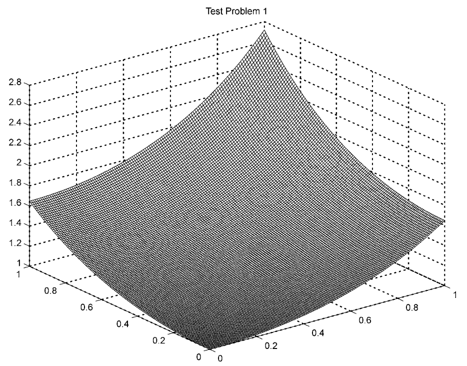

Fig. 1. Test problem 1: Graph of the computed solution.

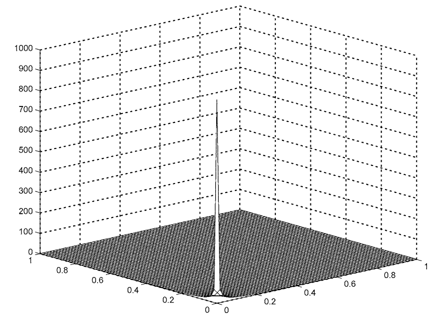

Fig. 2. Test problem 2: Graph of the right-hand side.

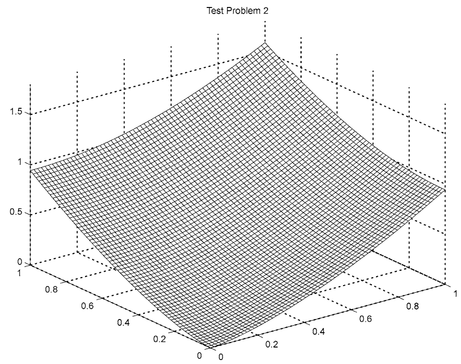

Fig. 3. Test problem 2: Graph of the computed solution.

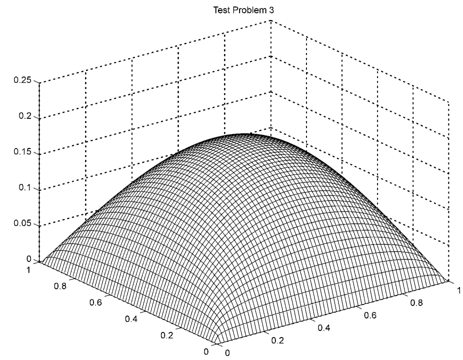

Fig. 4. Test problem 3: Graph of the computed solution.

$C^2(\overline{\Omega})$-regularity. When, after space discretization, we apply algorithm (8)–(11) to the solution of problem (14), we still observe $\mathrm{O}(h^2)$ for the $L^2(\Omega)$-approximation error. On Figs. 2 and 3 we have visualized, respectively, the graph of the right-hand side of Monge–Ampère equation in (14) and the graph of the computed solution corresponding to $h = 1/64$. The third test problem, namely (2), i.e.,

$$\det D^2\psi = 1 \quad \text{in } \Omega, \qquad \psi = 0 \quad \text{on } \Gamma, \tag{15}$$

is by far the most intriguing. Indeed, despite the fact that problem (15) has no solution in $H^2(\Omega)$, algorithm (8)–(11) produces a sequence $\{\psi^n\}_n$ converging (geometrically) to a limit ψ_h^c, while the sequence $\{\boldsymbol{\lambda}^n\}_n$ diverges (arithmetically). The graph of ψ_h^c, obtained with $h = 1/64$ has been shown on Fig. 4, while the intersections of this graph with the planes $x_1 = 1/2$ and $x_1 = x_2$ have been shown on Figs. 5 and 6, respectively, for $h = 1/32$, $1/64$, and $1/128$. A close inspection shows that the curvature of the graph becomes negative close to the corners, in violation of the Monge–Ampère equation; actually, it is also violated along the boundary, which is what we expected, since (with obvious notation), $\|D_h^2\psi_h^c - \mathbf{p}_h^c\|_{L^2(\Omega)} = 1.8 \times 10^{-2}$ if $h = 1/32$, 3.3×10^{-2} if $h = 1/64$, 4.2×10^{-2} if $h = 1/128$, while $\|D_h^2\psi_h^c - \mathbf{p}_h^c\|_{L^2(\Omega_1)} = 2.7 \times 10^{-4}$ if $h = 1/32$, 4.1×10^{-4} if $h = 1/64$, 4.9×10^{-4} if $h = 1/128$, and $\|D_h^2\psi_h^c - \mathbf{p}_h^c\|_{L^2(\Omega_2)} = 4.4 \times 10^{-5}$ if $h = 1/32$, 2.9×10^{-5} if $h = 1/64$, 5.1×10^{-5} if $h = 1/128$, where $\Omega_1 = (1/8, 7/8)^2$ and $\Omega_2 = (1/4, 3/4)^2$. Actually, since ψ_h^c does not vary very much with h, we suspect that, according to Remark 3.2, what we have here is a (good) approximation of one of these functions of V_0 whose Hessian is at a minimal L^2-distance (global or local) from the set Q_f introduced in Section 3.

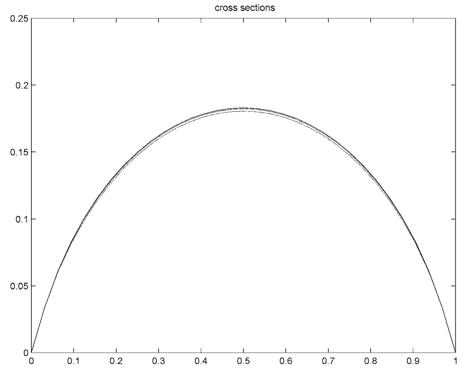

Fig. 5. Test problem 3: Graph of the solution restricted to the plane $x_1 = 1/2$.

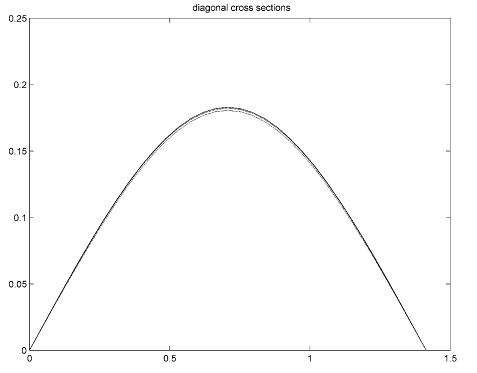

Fig. 6. Test problem 3: Graph of the solution restricted to the plane $x_1 = x_2$.

Remark 4.1. Following a suggestion of L. Caffarelli, we are presently investigating the solution of the *regularized Monge–Ampère equation*

$$\varepsilon \Delta \psi + \det D^2 \psi = f \quad \text{in } \Omega, \qquad \psi = g \quad \text{on } \Gamma,$$

by a variant of algorithm (8)–(11); the corresponding results will be reported elsewhere.

Acknowledgements

The authors want to thank Professors David Bao, Luis Caffarelli and Luc Tartar for, respectively, introducing us to Differential Geometry, Monge–Ampère and fully nonlinear elliptic equations, and (a very long time ago) to the weak continuity properties of Jacobian determinants. The invaluable help of P. Muscarello in the preparation of this article is greatly appreciated, as are the comments of Y. Brennier.

References

[1] T. Aubin, Nonlinear Analysis on Manifolds, Springer-Verlag, Berlin, 1982.
[2] L.A. Caffarelli, The Monge–Ampère equation and optimal transportation: an elementary review, Lecture at ICM 2002, Beijing, August 20–28, 2002.
[3] L.A. Caffarelli, X. Cabre, Fully Nonlinear Elliptic Equations, American Mathematical Society, Providence, RI, 1995.
[4] M. Fortin, R. Glowinski, Augmented Lagrangians, North-Holland, Amsterdam, 1983.
[5] R. Glowinski, P. Le Tallec, Augmented Lagrangians and Operator Splitting Methods in Nonlinear Mechanics, SIAM, Philadelphia, 1989.
[6] R. Glowinski, J.-L. Lions, R. Tremolieres, Numerical Analysis of Variational Inequalities, North-Holland, Amsterdam, 1981.
[7] V.I. Oliker, L.D. Prussner, On the numerical solution of the equation $z_{xx} z_{yy} - z_{xy}^2 = f$ and its discretization, I, Numer. Math. 54 (1988) 271–293.